Neutron Powder Diffraction Study of D_2 Sorption in Cu_3(1,3,5-benzenetricarboxylate)$_2$

Vanessa K. Peterson,[†] Yun Liu,[‡,§] Craig M. Brown,[‡,⊥] and Cameron J. Kepert[*,†]

School of Chemistry, The University of Sydney, NSW 2006, Australia, NIST Center for Neutron Research, Gaithersburg, Maryland 20899-8562, Department of Materials Science and Engineering, University of Maryland, College Park, Maryland 20742-2115, and Indiana University Cyclotron Facility, Bloomington, Indiana 47408

Received August 25, 2006; E-mail: c.kepert@chem.usyd.edu.au

The recent focus on hydrogen as an alternative energy carrier has led to the question of how to store hydrogen gas safely and efficiently. This question has arisen in parallel with the development of an important new class of nanomaterials that show outstanding promise in this area, porous metal organic frameworks. The exploration of the location of H_2 within these materials and their structural behavior during H_2 sorption is allowing the delineation of the structural features that maximize hydrogen loading, in turn providing fundamental insight into the structural behavior and porous nature of these materials.

$Cu_3(BTC)_2$, where BTC = 1,3,5 benzenetricarboxylate, is a three-dimensional cubic (*Fm*-3*m*) neutral coordination framework composed of dinuclear cupric tetracarboxylate units bridged by three-connecting BTC units to form a Pt_3O_4-type network.[1] The framework shows structural stability to complete desolvation and is stable to 250 °C. The Cu atoms in the fully dehydrated phase are coordinatively unsaturated; such sites are of interest in that they have been proposed to favor high dihydrogen binding enthalpies.[2−4] Hydrogen sorption data for this material at 77 K (Supporting Information) show values up to 2 wt % at 100 Pa, with saturation of just over 3 wt % achieved at 9×10^6 Pa.[5] At lower pressures (below ca. 1×10^6 Pa) $Cu_3(BTC)_2$ and MOF-74 show maximal H_2 uptake for coordination frameworks, a property that may arise from binding to open-metal sites with relatively high affinity for dihydrogen.[5,6] Here we reveal the location of six D_2 binding sites in $Cu_3(BTC)_2$, using neutron powder diffraction, and describe an intricate filling order of the framework. The most favored of these sites lies in close proximity to the open Cu sites.

$Cu_3(BTC)_2$ has a complex three-dimensional channel system. The largest pores are 9 Å in diameter and are formed from 12 dinuclear $Cu_2(OOC)_4$ subunits forming a cuboctahedron. A second pore system is accessible from these larger pores, in which four benzene rings constitute the inner surface with the centers of the rings forming a tetrahedron of diameter 5 Å. The triangular windows leading to these secondary pores are 3.5 Å in diameter.

$Cu_3(BTC)_2$ was prepared using a hydrothermal method (Supporting Information). Neutron powder diffraction data were collected on $Cu_3(BTC)_2$ in a vanadium can using the high-resolution neutron powder diffractometer (BT-1) at the National Institute for Standards and Technology Center for Neutron Research. Data were collected using neutrons with a wavelength of 2.0787 Å, from 2θ = 4° to 145°. D_2 was substituted for H_2 due to the large incoherent scattering of H. Gas quantities corresponding to D_2:Cu ratios of 0, 0.5, 1, 2, and 4 were loaded into the sample via a capillary line. Temperature control was achieved using a top-loading closed-cycle helium refrigerator. D_2 was loaded at 77 K and the sample cooled to 5 K before data were collected. Gas sorption was observed by

† The University of Sydney.
‡ NIST Center for Neutron Research.
§ University of Maryland.
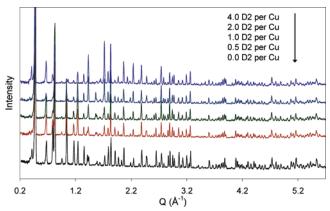⊥ Indiana University Cyclotron Facility.

Figure 1. Neutron powder diffraction data for $Cu_3(BTC)_2$ with adsorbed D_2.

monitoring the pressure in the control volume; total gas sorption was always achieved above 30 K.

Structural analyses were performed using Rietveld refinements using GSAS as implemented in EXPGUI.[7,8] Rietveld refinement was performed using the structural model of Chui et al.[1] with a 12-term cosine-Fourier series background function and the pseudo-Voigt peak profile with asymmetry (CW Type II in GSAS). The resulting crystalline model was used for the analyses of the powder diffraction data of $Cu_3(BTC)_2$ and then as the initial model for the D_2 adsorbed data with the D_2 locations derived from Fourier difference techniques. Two small reflections were unable to be indexed by the model. Given the high affinity of the framework for D_2 and the small amount of this contaminant phase, it is unlikely that this contaminant affects the measured D_2 sorption (Supporting Information).

The powder diffraction pattern was observed to change significantly during the D_2 loading (Figure 1). The crystalline lattice expands as D_2 is adsorbed, then contracts slightly at higher D_2:Cu loadings (Table 1). This contraction is associated with a subtle buckling of the BTC units and a concomitant decrease in the BTC-bridged Cu···Cu distance from 8.07(1) Å to 8.03(1) Å.

Rietveld analyses of the $4D_2$:Cu loaded sample revealed the location of six D_2 adsorption sites, each site representing the centroid of the D_2 molecule (Tables 2 and 3, Figure 2). The most favorable site, $D_2(1)$, shown on the left in Figure 3, occupies the coordinatively unsaturated axial sites of the dinuclear Cu center. This site is located 2.39(1) Å from the Cu atom (cf. Cu−OH_2 coordination bond distance of 2.17(1) Å in the hydrated material[1]), indicating there is significant interaction with the d^9 Cu(II) center. Notably, the binding distance is considerably greater than that of σ-bonded η^2-dihydrogen complexes, e.g., of group 6 metal ions (M−H ca. 1.7−2.0 Å).[9] This comparatively long interaction appears consistent with the reported observation of a high-energy ν(H−H) sideband in the IR spectra of H_2-loaded $Cu_3(BTC)_2$.[10]

Table 1. Lattice Parameter and Goodness-of-Fit Results for Rietveld Analysis Using Diffraction Data for $Cu_3(BTC)_2$ Loaded with D_2

D_2/Cu	lattice parameter (Å)	R_{wp} (%)	dWD
0	26.3046(2)	2.82	0.963
0.5	26.3159(3)	3.17	1.118
1	26.3256(3)	3.51	0.945
2	26.3214(3)	3.58	0.898
4	26.3136(4)	3.77	0.959

Table 2. Refined Parameters for D_2 Binding in $Cu_3(BTC)_2$ at the $4D_2$:Cu Loading

site	x	y	z
$D_2(1)$	0.1515(2)	0.1515(2)	0
$D_2(2)$	0.25	0.25	0.312(2)
$D_2(3)$	0.1556(4)	0.1556(4)	0.1556(4)
$D_2(4)$	0.3714(4)	0.1286(4)	0
$D_2(5)$	0.2056(7)	0.2056(7)	0.2056(7)
$D_2(6)$	0.2821(6)	0.0756(6)	0

Table 3. D Site Occupations (where SOF is for D_2) and Rietveld Calculated Quantities as a Function of D_2 Loading for $Cu_3(BTC)_2$

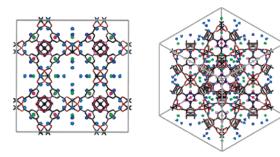| D_2:Cu	$D_2(1)$ SOF	$D_2(2)$ SOF	$D_2(3)$ SOF	$D_2(4)$ SOF	$D_2(5)$ SOF	$D_2(6)$ SOF	calc D_2:Cu	calc wt % H_2
0.5	0.94(2)	0.05(1)					0.50(1)	0.50(1)
1	1.80(2)	0.16(1)					0.98(3)	0.98(3)
2	2.02(2)	0.37(1)	2.11(3)				1.90(2)	1.90(2)
4	1.99(2)	0.38(3)	2.12(4)	1.69(3)	0.78(5)	1.39(2)	4.39(5)	4.40(4)

Figure 2. D_2 in $Cu_3(BTC)_2$ shown along the [001], left, and [111], right, directions. D_2 sites are represented as spheres and are color coded to match Figure 3.
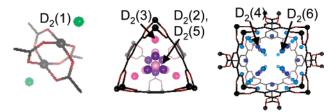

Figure 3. D_2 sites in $Cu_3(BTC)_2$: axial Cu site (left); view along [111] in the 5 Å small pore with 3.5 Å side windows (middle); and view along [100] showing the 9 Å pore.

The order of filling of subsequent sites is sequential from $D_2(2)$ to $D_2(6)$ (see Table 3 and Figure 3). Following binding at the metal sites, there is a progressive occupation of the $D_2(2)$ site, which lies within the 5 Å pores at a distance 3.29(1) Å from a benzene ring of the BTC unit. The 3.5 Å windows accessing these pores are next to fill, with the $D_2(3)$ site residing in the center of these windows 3.88(1) Å from six BTC oxygen atoms and 3.90(1) Å from three BTC carbon atoms. Analysis of the 4 D_2:Cu phase shows partial occupation of three further sites at higher loading: $D_2(4)$ lies 3.31(1) Å from two BTC carboxylate carbon atoms within the 9 Å pores; $D_2(5)$ lies 3.63(1) Å from three BTC benzene carbon

atoms within the 5 Å pores; and $D_2(6)$ lies 3.23(1) Å from two BTC carboxylate oxygen atoms within the 9 Å pores. The filling of smaller, then larger, pores is consistent with the theory of micropore filling.[11] These results complement previous grand canonical Monte Carlo simulations performed in conjunction with high-resolution low-pressure Ar sorption experiments, which indicated a graduated pore-filling sequence beginning with the smaller pores, followed by a stepwise adsorption and condensation in the main pores.[12] High-resolution N_2 isotherms for this material also correspond to the filling of the narrower, then larger, pores.[13]

Analysis of the D_2 site-to-site distances within the 5 Å pores indicates that at most two of the six octahedrally arranged $D_2(2)$ sites may be occupied (corresponding to a D_2 SOF of 0.67), these lying 3.27(1) Å from each other (cf. an unphysical 2.31 Å for neighboring sites). It seems likely that progressive filling of this pore from two to three D_2 molecules would then involve depopulation of one of these $D_2(2)$ sites and occupation of two of the four tetrahedrally arranged $D_2(5)$ sites such that $D_2(2)\cdots D_2(5) = 3.26$-(1) Å and $D_2(5)\cdots D_2(5) = 3.30(1)$ Å. The refined site occupancies (Table 3) for the $4D_2$:Cu loaded sample are consistent with ca. 80% of the pores containing three D_2 and ca. 20% containing only two. Further data collection is planned to explore competitive D_2 site filling at high D_2:Cu loadings.

In conclusion, we demonstrate the progressive filling of six distinct D_2 sites within the nanopore structure of $Cu_3(BTC)_2$. Location of the primary site at the coordinatively unsaturated Cu atoms provides direct structural evidence of the potential importance of such metal sites to hydrogen storage. Competitive loading of the other D_2 sites proceeds with the pores filling from smallest to largest. It is likely that at saturation more D_2 can be incorporated, most likely leading to more complete filling of both the 5 and 9 Å pores.

Supporting Information Available: Synthesis; crystallographic data including structural results for Rietveld analysis using diffraction data for $Cu_3(BTC)_2$ loaded with D_2; H_2 and N_2 sorption data. This material is available free of charge via the Internet at http://pubs.acs.org.

References

(1) Chui, S. S.-Y.; Lo, S. M.-F.; Charmant, J. P. H.; Orpen, A. G.; Williams, I. D. *Science* **1999**, *283*, 1148−1150.
(2) Chen, B.; Ockwig, N. W.; Millward, A. R.; Contreras, D. S.; Yaghi, O. M. *Angew. Chem.. Int. Ed.* **2005**, *117*, 4823−4827.
(3) Chapman, K. W.; Southon, P. D.; Weeks, C. L.; Kepert, C. J. *Chem. Commun.* **2005**, 3322−3324.
(4) Kaye, S. S.; Long, J. R. *J. Am. Chem. Soc.* **2005**, *127*, 6506−6507.
(5) Wong-Foy, A. G.; Matzger, A. J.; Yaghi, O. M., *J. Am. Chem. Soc.* **2006**, *128*, 3494−3495.
(6) Rowsell, J. L. C.; Yaghi, O. M. *J. Am. Chem. Soc.* **2006**, *128*, 1304−1315.
(7) Larson, A. C.; Dreele, R. B. V. *General Structure Analysis System (GSAS)*; Los Alamos National Laboratory Report; LAUR, 2000; pp 86−748.
(8) Toby, B. H. *J. Appl. Crystallogr.* **2001**, *34*, 210−213.
(9) Kubas, G. J. *J. Organomet. Chem.* **2001**, *635*, 37−38.
(10) Prestipino, C.; Regli, L.; Vitillo, J. G.; Bonino, F.; Damin, A.; Lamberti, C.; Zecchina, A.; Solari, P. L.; Kongshaug, K. O.; Bordiga, S. *Chem. Mater.* **2006**, *18*, 1337−1346.
(11) Rouquerol, F.; Rouquerol, J.; Sing, K. *Adsorption by Powders & Porous Solids*; Academic Press: San Diego, 1998.
(12) Vishnyakov, A.; Ravikovitch, P. I.; Neimark, A. V.; Bulow, M.; Wang, Q. M. *Nano Lett.* **2003**, *3*, 713−718.
(13) Krawiec, P.; Kramer, M.; Sabo, M.; Kunschke, R.; Fröde, H.; Kaskel, S. *Adv. Eng. Mater.* **2006**, *8*, 293−296.

JA0660857